Uncertainty analysis as a tool for refining land dynamics modelling on changing landscapes. A study case in a Spanish Natural Park

Jose-Manuel Álvarez Martínez [a] *,
Jetse J. Stoorvogel [b],
Susana Suárez-Seoane [a] and
E. de Luis Calabuig [a]

[a] Área de Ecología, Fac. CC. Biológicas y Ambientales, 24071 Campus de Vegazana, Universidad de León, León, Spain

[b] Land Dynamics Group, Wageningen University, P.O. Box 37, 6700 AA Wageningen, The Netherlands

* Corresponding author. E-mail address: jm.alvarez@unileon.es (J.M. Álvarez-Martínez).

Abstract

In this work, we developed a RS-based methodology aimed at improving the assessment of inter-annual land cover dynamics in heterogeneous and resilient landscapes. This is the case of the Spanish Natural Park of Sierra de Ancares, where human interference during the last century has resulted in the destruction and fragmentation of the original land cover. A supervised classification with a maximum likelihood algorithm was followed by an uncertainty assessment by using fuzzy classifications and confusion indices (CI). This allowed us to show how much of the study area contains a substantial amount of error, distinguishing data that might be useful to measure land change from data that are not particularly useful, and therefore to detect true changes not skewed by the effects of uncertainty. Even if patterns of change were always coherent among images, they were more realistic after reducing uncertainty, although the number of available pixels (i.e. unmasked by the method) decreased substantially. Using these data, we modelled land cover dynamics by using a program specifically created to determine the frequency of disturbances (mainly fire events), or recurrence, and the vegetation recovery time during the study period. The model outputs showed correlated landscape patterns at a broad scale and provide useful results to explore land cover change from pattern to process.

Keywords: Land cover change; Remote sensing; Uncertainty; Fuzzy classification; Confusion Index; Recurrence; Vegetation recovery

1. Introduction

Land cover mosaics are highly dynamic at varying spatio-temporal scales as a result of the contrasting effects of both anthropogenic and natural disturbances and vegetation recovery processes (Burgi et al. 2004; Lambin et al. 2001). In human-dominated landscapes, disturbances such as fire (Lozano et al. 2008; Lloret et al. 2002), deforestation or overgrazing (Duveiller et al. 2008; Rees et al. 2003), in addition to land abandonment (Benayas et al. 2007; MacDonald et al. 2000), drive the dynamics of land cover patterns and the associated processes. Therefore, during recent decades, an increasing number of spatially-explicit methodologies have been developed to provide a better knowledge of past-to-present land cover changes at a regional scale (Stoorvogel and Antle 2001; Verburg et al. 2002). Many of these methods are based on remote sensing (RS) techniques (Roder et al. 2008; Treitz and Rogan, 2004), since they provide regional data at different temporal scales with low collection effort. However, although RS has in some cases been presented as an easy tool for deriving land cover inventories, the images require the application of complex and laborious procedures, including pre-processing (for geometric, radiometric, atmospheric and topographic corrections) and classification tasks. The correct implementation of all these steps plays an important role in the reliability of the final characterizations (Fuller et al. 2003).

The most commonly used land cover classifier is maximum likelihood (Maxlike) (Conese and Maselli, 1992; Martin et al. 1998; Shalaby and Tateishi 2007), which produces a hard classification based on simple statistical principles. This technique has shown satisfactory results in various applications, improving on other procedures (Carvalho et al. 2004; Rogan et al. 2002), and it has been widely used because of its easy implementation. However, classifications derived from Maxlike often still result in

an approximate error of 20% (Liu et al. 2007; Treitz and Rogan 2004). This level of misclassification may be acceptable if the study is carried out on a single image, but it may seriously affect land cover change studies based on multiple images (Pontius et al. 2004). It is therefore interesting to develop complementary methodologies to improve the interpretation of the resulting land cover maps obtained by means of this technique.

Since classifications remain simplifications of real landscapes (Woodcock and Gopal 2000), the product of image classification always contains an element of uncertainty (Metternicht, 2003; Steele et al. 1998). Moreover, as the sequence of land covers actually constitute a continuum; the assignment of a particular category to a pixel will always generate a certain degree of confusion (Lewis et al. 2000; Bradley and Mustard 2005) that must be evaluated (Wang and Howarth 1993). This issue has been analyzed previously, often on the basis of the fuzzy k-means classification (Ahamed et al. 2000; Foody 1996), which is a well-established method used to map mixed units emerging in heterogeneous landscapes. However, although these techniques have been used in vegetation (Tapia et al. 2005), soil (Burrough et al. 1997), urban expansion (Zhang and Foody 1998) and forestry studies (Triepke et al. 2008), they have not been specifically applied in landscape dynamics assessment as presented in this work. In fact, most of the land cover change analyses found in the literature are based only on comparisons among a limited number of images over a larger period (Cayuela et al. 2006; Gautam et al. 2003; Xiao et al. 2006). However, in changing human-dominated territories, processes which control landscape dynamics should be assessed on a yearly basis in order to detect all land cover changes and to avoid misunderstanding the real patterns within a landscape (Diaz-Delgado and Pons 2001; Lloret et al. 2002; Wilson and Sader 2002).

In this context, we studied inter-annual land cover changes in a Spanish Natural Park over the last fourteen years, using remote sensing techniques. We developed a methodology based on fuzzy classifications and confusion indices to identify the pixels where the classification and change detection is less accurate, because of the effect of uncertainty. Those pixels are then sequentially excluded from the further land cover change analyses in order to evaluate its potential increase in reliability. Finally, to illustrate the approach, we analyzed the series of land cover maps, with and without uncertainty, by means of a model developed specifically to assess the frequency of disturbances (mainly fire events) and vegetation recovery time.

2. Methods

2.1 Study area

La Sierra de Ancares is a Natural Park of the Autonomous Region of Castilla y León (Spain) located at the western extreme of the Cantabrian Mountains. It covers approximately 100,000 ha, which include two protected areas by the Nature 2000 Network (92/43/EEC): Sierra de Los Ancares and Alto Sil (Figure 1). Recently, it was also declared a UNESCO Biosphere Reserve to preserve outstanding ecological values, such as habitats suitable for brown bear (*Ursus arctos*) and capercaillie (*Tetrao urogallus cantabricus*). The elevation ranges from 600 to 2200 meters of altitude and coincides with moderate to steep relief. Climatically, the area is dominated by an Atlantic climate with a mean annual precipitation of 1300 mm and a mean temperature of 8°C (Ninyerola et al. 2005), although the lower altitudes show sub-Mediterranean characteristics.

Land cover experienced major changes in the past, and currently exhibits a fragmented pattern. Human interference during the last century has resulted in the fragmentation of the original forest cover, coinciding with extensive tree fellings from the 1940s to 1970s. During recent decades, the depopulation of rural areas has involved the disappearance of agriculture and livestock farming, reforestation and the invasion of old fields by shrubs and forests. Although pasture maintenance is not necessary under current forestry policies, deliberate burning is still continued. Burning takes place mainly during summer (from June to September), and is the main problem for wildlife maintenance, together with a significant mining industry, which is especially important in Alto Sil.

2.2 Input data and pre-processing

Fourteen Landsat TM and ETM+ images were acquired on a yearly basis (from 1991 to 2004) for the study area (Table 1). We selected images from the end of summer to the beginning of autumn to allow for proper comparisons (avoiding major changes in vegetation phenology), and to ensure the collection of burned areas, a minimum cloud cover and a relatively high sun elevation. Nevertheless, image availability and cloud presence compelled us to acquire three images from early June/July. In addition, a complementary digital elevation model (DEM) was developed following a stereo-matching technique from equidistant points derived digital aerial photographs obtained in 2004, at a scale of 1:5000. This DEM was resampled at 30 metres resolution to match the Landsat images. The model is reliable, as was concluded by a validation assessment with field data, and has already been used successfully in other environmental studies (Lozano et al. 2008; Prieto, pers. com.).

The images were geometrically corrected by means of a second-order polynomial (Pala and Pons 1995) using 60 ground-control points per image, producing an average root mean square error of 20.1 m for the Landsat TM images and 11.8 m for the ETM+ images. This method is effective in mountainous regions since it incorporates the DEM developed to allow close adjustment for topography. We applied the Nearest Neighbour Algorithm to keep the original values of pixels unchanged. The sub-pixel georectified images were then radiometrically corrected using the algorithms proposed by Markham and Barker (1987) and Moran et al. (1992). The COST model (Chavez 1996) was applied for atmospheric correction. Down-welling transmittance values for bands five and seven were taken from Gilabert et al. (1994), since their study area had similar atmospheric conditions to ours. Finally, a topographic correction was applied with the C correction model (Riaño et al. 2003; Teillet 1986) to compensate for different solar illuminations due to the mountainous character of the area. As each individual image was classified independently, we did not carry out a normalization of the time series. The methods and algorithms used for correcting the images were the same than used in Lozano et al. (2008).

2.3 Classification of satellite images

After several exploratory analyses (i.e. regression and non-supervised classification followed by cluster analyses) for determining homogeneous land cover categories on study area, a supervised classification using a maximum likelihood algorithm (Maxlike) was conducted on a per-pixel based approach, for each of the 14 available images. Seven major land cover classes were recognized: (1) broadleaf woodlands dominated by various species of oaks (*Quercus pyrenaica*, *Q. robur* and *Q.*

petraea) or birches (*Betula sp.*), and riverside forests. (2) Meadows with hedges and farmlands in the valley bottoms. (3) Shrublands and heathlands (*Erica spp*, *Chamaespartium tridentatum, Calluna vulgaris, Cytisus spp*. and *Genista spp*., in order of importance), where conifer reforestation by human planting occurs. (4) Rock outcrops and dry subalpine-alpine climatic pastures. (5) Bare land, mostly resulting from fire events and, in minor proportion, mines, quarries and shrub-clearings. (6) Water surfaces. (7) Urban patches (towns, villages and isolated farms). Water surfaces and urban patches were considered constant (and then digitalized on screen), because of their scarce representation (less that 1% of study area) and low values of change at a broad scale through the study period. Therefore, classification focused on the five remaining change categories from the seven described before. It was based on: (1) bands 1-7 of the Landsat images, excluding thermal band 6 because of its different spatial resolution and spectral characteristics, not allowed by the models used in the radiometric correction; (2) the Normalized Differenced Vegetation Index (NDVI) (Rouse et al. 1973) and the component ”greenness” of the Tasselled Cap Transformation (Kauth and Thomas 1976), as a measure of total photosynthesis and the productivity of vegetation; and (3) elevation and slope.

Training areas were identified on-screen using a seed pixel (region growing) approach (Lillesand et al. 2008). A total of 200 “clouds of pixels” consisting of 50 pixels each (4.5 ha) were determined independently for each image. To ensure that all spectral classes constituting each information class (land cover category) were statistically sampled, representing its spectral variability in the image, the number of areas per land cover unit increased with increasing heterogeneity (i.e. the nature of the information class sought-after) and the complexity of the geographic area under analysis (Lillesand et al. 2008). Thus, broadleaf forests accounted for the greatest number (100),

while shrublands had 40 and meadows, rock outcrops and bare land categories accounted for 20 each. The selection was aided by using information derived from field work during the year 2004 and high spatial resolution digital aerial photographs from 1991, 1997, 2000 and 2004 (provided by the Regional Government of Castilla y León). When no source of ground-truthed information was available, analysis based on the visual training acquired during the image interpretation supported by the information sources, was used to develop the reference dataset (Chuvieco 2000).

2.4 Accuracy and uncertainty

The problem of accuracy in multi-temporal datasets

In assessing land cover change with multi-temporal datasets, a variety of factors influences the accuracy of the products through misregistration (i.e. differences in boundary locations, or positional error) (Dai and Khorram 1998; Roy 2000) and misclassification (i.e. erroneous allocations made by conventional (hard) classifiers on mixed pixels, or classification error) (Bradley and Mustard 2005; Cherrill and McClean 1995), as well as the interaction of both over time (Burnicki et al. 2007; Carmel et al. 2001). The effect of topography is also important, since a larger error has been associated with north-facing aspects and steeper slopes (Carmel 2004), although this is only true for northern hemisphere areas at higher latitudes. Finally, radiometric and atmospheric effects can also affect classification accuracy (Carmel et al. 2001), as atmospheric attenuation and sometimes the radiometer or its conditions may vary.

Irrespective of their origin, the spatial variability of error can be a major concern in change-detection (Foody 2002). When multiple data-layers are involved, the majority

of this error is not randomly distributed over the study area, but spatially correlated at the boundaries of classes, i.e. the edges of land cover patches (Edwards and Lowell 1996; Steele et al. 1998). Unfortunately, the confusion matrix and the accuracy metrics derived from it provide no information on the spatial distribution of error (Canters 1997; Steele et al. 1998), which is crucial for proper interpretation (Pontius and Lippitt 2006). Thus, together with the accuracy assessment, some kind of spatially-explicit representation of the uncertainty of the classified maps (i.e. all type of errors acting as a whole) would be useful for making reliable predictions about landscape dynamics. This article discusses uncertainty introduced to the data by the characteristics of the land cover classes of interest, specifically resulting from spectral confusion and from image resolution (Lewis et al. 2000). Other sources of uncertainty, such as positional uncertainty, are beyond the scope of this work.

Accuracy assessment of maps: ground information and confusion matrix

The accuracy of the land cover maps developed for only 1991, 1997, 2000 and 2004 could be assessed because of the limited availability of ancillary data (field verification and digital aerial photographs), which provided the required ground information. An individual set of test data was developed for each year.

To determine the test sampling unit for a pixel-based classification, Janssen and Van der Vel (1994) stated that individual pixels were the most appropriate dataset. Nevertheless, as pixels are usually uniform in shape and size, represent small areas in Landsat images (30 m) and partition the mapped population into a finite, though large, number of sampling units, they are related to point sampling units. Thus, following a site-specific accuracy assessment procedure, a total of 300 testing points were selected

for the years 1991, 1997 and 2000. For 2004, the reference year for the image series, up to 1325 points were field-checked to assess the reliability of the results more rigorously. A stratified random sampling was applied to ensure that each class was represented by at least 50 points for collecting all the variability in the information classes. Points were selected using a 3x3 kilometers moving window. Each accuracy assessment point was then examined to ensure that it did not fall within the associated class of interest's training regions; any point that did was replaced.

The testing points were used to construct confusion matrices (Congalton 1991), using standard accuracy assessment methods (Stehman and Czaplewski 1998). These provided a global summary of: (1) overall accuracy, or an overall measure of the quality of a map; (2) producer's accuracy or omission errors, as a measure of real pixels not included in the correct land cover class; and (3) user's accuracy or commission errors, a measure of the pixels erroneously classified as a particular land cover (Stehman 1997). Some general level of accuracy is typically specified as a target against which the classification may be evaluated (Foody 2002). In general terms, overall accuracies of 80-90% are commonly recommended (Liu et al. 2007; Thomlinson et al. 1999), although this threshold actually depends on the complexity of the study area and the objectives of the work (Rogan et al. 2002).

Additionally, official fire occurrence statistics available at the Regional Government of Castilla y León for the entire study period (1991-2004), were analyzed to assess the contribution of fire events to the bare land category. The total area burned (and the number of fire events) per year, extracted for the study area from the statistics, were correlated with the area covered by bare land on the classified images, through a Spearman test for non-parametric data. The number of observations (n) was fourteen (one for each year of study period) and the unit of observation was the percentage of

area burned (or number of fire events) for each point in time. In addition, complementary fieldwork and visual analyses of the high spatial resolution digital photographs were carried out.

Uncertainty assessment of error: fuzzy classification and confusion index

The likelihood rule classifies pixels in the land cover class with maximum membership probability, although they could have an almost equal probability of membership to another class (Lewis et al. 2000), which defines the uncertainty associated to the classification process. To assess the uncertainty derived from these erroneous allocations made by conventional (hard) classifiers, a methodology based on fuzzy k-means memberships was applied to the classification results (Owen et al. 2006). This method yields membership probabilities for each of the land cover classes which can be used to calculate a Confusion Index (CI) as a measure of classification uncertainty (Burrough et al. 1997). The CI distinguishes subareas with high uncertainty due to class overlapping (which occurs mainly at boundaries between categories) from those with low uncertainty (e.g. pure pixels), accepting that one pixel can belong to more than one class (Tapia et al. 2005). In the fuzzy k-means classification, a measure of distances to the class centre (d_c) is calculated for each pixel. The similarity measure between the vector (x_s) (the characteristics at a particular pixel *s*, where characteristics refer to the digital values for each band included in the classification procedure for that particular pixel *s*) and the representative vector of the land cover class *c* (μ_c) is determined by the normalized Euclidean distance as follows:

$$d_c = \sqrt{\sum_{i=1}^{n} \left((x_{s,i} - \mu_{c,i}) / sd_i \right)^2} \qquad \text{(Eq. 1)}$$

where sd_i stands for the overall standard deviation of characteristic i, and n is the number of bands used in the classification procedure.

A small d_c indicates that x is similar to the land cover class c, whereas a large d_c indicates large differences. Using these distances, the fuzzy membership grade of one pixel for a suitability class c (p_c) is given by Eq. 2, where m is the number of land cover classes:

$$p_c = d_c / \sum_{j=1}^{m} d_j \qquad \text{(Eq. 2)}$$

The confusion associated with the classification of a pixel can be expressed by the Confusion Index (CI) given in Eq. 3, where pc(max) is the membership value of the class with the maximum p_c for that pixel and pc(max-1) is the second-largest membership value for the same pixel.

$$CI = \left(1 - (p_c(\max) - p_c(\max - 1))\right) \qquad \text{(Eq. 3)}$$

If one class clearly dominates above the others (CI approaches 0), there is little confusion in the classification process for that pixel. If CI approaches 1, then both p_c-values are similar and there is confusion as to the land cover class to which the pixel certainly pertains.

For each of the 14 classified images, a map with the CI was calculated. Subsequently, in addition to the original land cover maps where all pixels were considered (CI 100 maps), we created land cover maps with 75% of the pixels which showed the lowest Confusion Index (CI 75 maps) and with 50% of these pixels (CI 50 maps). Classification errors will be progressively masked from the map series as the method increases in accuracy and coherence (i.e. similarity) between images. Thus, the most reliable land cover dynamics could be determined by using only those pixels classified with the lower uncertainty.

All analyses were undertaken using ArcGIS 9.2 (ESRI 2006) and ERDAS IMAGINE 8.5 (ERDAS 2001).

2.5 Land cover dynamics

Firstly, the temporal evolution of each land cover category and the Spearman correlations between them were analyzed. The number of observations (n) was fourteen (one for each year of study period) and the unit of observation was the percentage of area covered by any particular category for each point in time. Secondly, land cover change was analyzed through post-classification comparison (Lambin 1999). All pair-wise images, also considering uncertainty, were studied using transition error matrices (van Oort 2007), which allowed an assessment of the nature and rate of land cover changes. The Spearman correlation between some changes was also assessed. The number of observations (n) was thirteen (one for each pair of years of study period) and the unit of observation was the percentage of area changing between both maps.

Once analyzed, the most important changes were quantitatively validated. The amount of change in relation to the increase in forest cover (represented by the transition from shrubland to forest) was compared with data available from the successive National Forestry Inventories of Spain (NFI) (Area of Environment, Ministry of the Environment and Rural and Marine Affairs, Government of Spain) and the Forest Atlas of Castilla and León (Gil Sánchez and Torre Antón 2007). Moreover, the total area burned (represented by changes from all vegetated land covers to bare land, while transitions from rock outcrops to bare were mainly related with new mines and quarries), was compared with data extracted from the official fire occurrence statistics of the Regional Government, for the period 1991-2004. Analyses were carried out for

the entire area (CI 100 maps), but also for maps retaining 75% (CI 75 maps) and 50% (CI 50 maps) of the most certainly classified pixels.

Subsequently, we analyzed land cover dynamics through the dataset of empirical observations (i.e. all the unmasked pixels of the classified images), by using a model specifically programmed by the authors. The model analyzes the dynamics along study period of each individual pixel and determines when, where and how often a particular land cover change takes place. This transition can include two different categories: original land cover (LC_A), in year *i*, and new land cover after change (LC_B), in year *j*; with *i, j* representing two years of study period such as $i < j$ (in advance sequence *A_B*). A bigger number of land covers can be included in the model, creating more complex sequences (e.g. LC_A remaining constant in years *i* and *i*+1, followed by LC_B in years *j* and *j*+1; with *i, j* representing two years of study period such as $i+1 < j$; in advance sequence *AA_BB*). In addition, the model allows for the calculation of the duration of a particular change (e.g. the time it takes for a burned pixel to recover into the original vegetation type). The output consists of a spatially-explicit representation for each of the model parameters: (i) year of first and last land cover change occurrence, (ii) number of times that a particular change occurs on the same pixel during study period, from an original land cover (LC_A) to another (LC_B) (or recurrence), and (iii) duration of any particular land cover change, since the year it happens (appearing LC_B) until the year of recovery to the original land cover class (LC_A) (time for vegetation recovery). In this work, we applied the model on sequences *A_B* and *AA_BB* using two parameters: change recurrence and time for vegetation recovery. To illustrate the effect of uncertainty, analyses were applied on the three levels of classification uncertainty (CI 100, CI 75 and CI 50 maps). Only pixel-strings with observations for all years were included in the modelling. Thus, when any pixel on any map is eliminated by the

363 uncertainty assessment, no observations for that particular location (i.e. the location of
364 the pixel masked) were considered in the analyses.
365

366 3. Results and Discussion

367

368 3.1 Classification accuracy

369

370 **Hard classification**

371

372 All maps for the whole temporal series showed a common pattern of land cover,
373 with different landscape elements spread out over a matrix of shrublands (see Figure 1a
374 for a representation of the maps for the first and last years). Due to its lower disturbance
375 regime (mainly less fire events), Alto Sil was more extensively covered by forest than
376 the Sierra de Los Ancares, where isolated patches of mature forest were relegated to
377 head-water basins. Valley bottoms were associated with hedged meadows and
378 farmlands, while bare land patches and rock outcrops appeared scattered throughout the
379 whole area, frequently mixed with fragmented heathlands at higher altitudes and on
380 slopes.

381 Table 2 provides the classification accuracy for the validation years. The overall
382 accuracy was consistently above 80%. The highest values were found in 2000 and the
383 lowest in 1991. These differences could be related to: (1) variation in the quality of
384 calibration data and image sensors between years; (2) confusion between real changes
385 and phenological differences in vegetation, cropping and changes in soil moisture
386 within the same land over type, associated with the acquisition date; and (3) limitations

in the classification procedure due to the spectral overlapping between categories (spectral uncertainty).

In general terms, the producer's accuracy was relatively lower in non-vegetated areas (where it was difficult to distinguish between rock outcrops and bare land) than in meadows, forests or shrublands. Nevertheless, this problem was expected given the difficulties of classifying land covers which share similar spectral response patterns from images relating to the dry season. Moreover, rock outcrop category aggregated a continuous gradation from non-vegetated surfaces to mixed heathlands on rocky places, which makes it difficult to identify pure patches. A similar problem appeared when classifying bare land, particularly in areas affected by fire events. In this case, there was confusion between recently burned areas, rock and shrublands, probably due to heterogeneous patterns in vegetation recovery after disturbance and fire severity (Diaz-Delgado et al. 2003; Lozano et al. 2007). Even so, the area of bare land category during study period was significantly correlated (Spearman coefficient) with data on area affected (r^2=0.31, $p< 0.05$; n=14) and number of wildfires (r^2=0.35, $p< 0.05$; n=14) of study area, obtained from the official fire statistics of the Regional Government. This result indicates that fire events contribute substantially to this land cover class.

The user's accuracy showed similar patterns, especially in the overestimation of non-vegetated surfaces. In particular, large areas of bare land and rock outcrops appeared mixed because of spectral confusion. Broadleaf forests and shrublands had, in general terms, the highest accuracy values, while meadows outside valleys were sometimes confused with forests or shrublands.

Analysis of uncertainty

412 Confusion index maps (see Figure 2) showed clear regional differences across
413 the study area. The highest confusion was associated with non-vegetated areas (i.e. rock
414 outcrops and bare land) by the reasons given before, while forests and meadows had the
415 lowest values and shrublands showed an intermediate situation (see Figure 1b and 1c for
416 a representation of the maps for the furthermost years). The overall pattern of
417 uncertainty was consistent for the whole temporal series, even if certain inter-annual
418 differences were detected, corresponding to real land cover changes. But how to
419 interpret this confusion index map?. As an example, if a fire event occurs in one year in
420 pixels classified as shrubland, these pixels will be certainly classified as bare land that
421 year. The CI of the map will be low. Nevertheless, after a period of time, depending on
422 fire severity and vegetation recovery patterns, the spectral characteristics of those pixels
423 vary, becoming closer to other categories (with herbaceous vegetation or even heathers)
424 and it results in confusion. Thus, the CI value of those pixels burned would increase,
425 becoming closer to one, and the probability of being masked by the uncertainty
426 assessment would also higher. Nevertheless, after reducing uncertainty, the area of bare
427 land continued to be significantly correlated, even at higher values (r^2=0.36, $p< 0.05$;
428 n=14), with data on the area and number of wildfires obtained from the official fire
429 statistics of the Regional Government. Furthermore, complementary fieldwork and
430 visual interpretation of aerial photographs provided an estimate that around 60% of the
431 bare areas were related to fires and 40% to mines, quarries, shrub-clearings, as well as
432 the effects of shadows on rock outcrops.

433 The elimination of pixels with the higher values of confusion index increased
434 maps accuracy (Table 3a), although the number of available pixels decreased
435 noticeably. Where the CI 100 maps had 86.75% of overall accuracy (mean value for the
436 four validated years), CI 75 showed 89.75% and CI 50 reached 92.50%. As a result, we

obtained maps composed of a lesser number of more reliable pixels spread throughout the area. Assuming temporal independence of error in individual classifications, the overall accuracy of a change map can be approximated by multiplying the individual overall accuracies of each classified image (Burnicki et al. 2007). In this work, as mentioned, because of the limited availability of ground-based information sources, we could assess only the accuracy of four non-consecutive maps, which allowed to creating and validating three change maps (Table 3b). The overall accuracy in all cases increased meaningfully after applying the CI, since the overall accuracy of the independent maps also increased. Consequently, the overall coherence (or similarity) of all pair-wise transition matrices increased after reducing the study area by eliminating the most uncertain classified pixels. It improved from 78.70% (average value with CI 100 maps) to 85.36% (with CI 75 maps) and 92.12% (with CI 50 maps). To clearly demonstrate the importance of incorporating uncertainty into the accuracy of the resulting change maps, all land cover changes computed for 1999-2000 are presented in Figure 4. The full difference image (Figure 4a) shows changes distributed all across the study area, affecting 25% of pixels of the whole map. Figures 4b and 4c, which represent an area more certainly classified, illustrate a diminishing amount of change (17% and 8% with CI 75 and CI 50 maps, respectively), giving a more realistic pattern. Nevertheless, the loss of pixels (or information) could imply an underestimation of the real amount of land change, as is demonstrated below.

3.2 Trends of change in landscape patterns

Hard classification

462 The temporal evolution of land cover classes between 1991 and 2004 is
463 presented in Figures 1a and 3a. Global changes were gradual through the study period,
464 with no major trends. Shrublands were, in all cases, the dominant land cover, reaching
465 maximum values in 1992, 1994, 1997 and 2002, which correlates with minima for non-
466 vegetated areas (r^2=-0.59, $p<0.01$; n=14). This indicates that fire events mainly occur in
467 shrub vegetation. Even with the appearance of new mining and quarries since 1995 in
468 Alto Sil, bare land slightly decreased through the years (r^2=-0.37, $p<0.05$; n=14),
469 probably because the widespread occurrence of fire events diminished and burned areas
470 were quickly colonized by heather communities. Forest cover was detected as relatively
471 higher in 1994 and 1999, probably due to the effect of the date of image acquisition
472 (beginning of June and July, when the consequences of summer drought were less
473 visible on vegetation). Hedged meadows and farmlands were the most stable land cover
474 type, showing variations of around 1% between years.

475 Table 4 (CI 100) shows that 21.3% of the area changed land cover every year
476 (on average for the study period), with different rates of gains and losses between land
477 covers. Six major changes accounted for 78.2% of the computed transitions. They
478 affected the following categories, in both directions of change: (1) forests and
479 shrublands, related with successional processes affecting diffuse boundaries; (2)
480 shrubland and rock outcrops, mainly associated with rapid recovery of vegetation after
481 disturbance and spectral uncertainty in sparse heathlands, and (3) shrublands and bare
482 land, where wildfires, shrub-clearings, mines and quarries cause vegetation losses over
483 large areas, followed by subsequent recovery. We also detected some changes that are
484 highly unlikely, such as the transition from rock outcrops to forest, which were related
485 to errors.

Table 4 (CI 100) also shows that changes from shrubland to forest occur yearly across 3.76% of study area, involving an increase in forested areas. Nevertheless, several studies have shown that in Central Western Spain the forested area has increased 30,000 ha $year^{-1}$ over the last three decades (Gil Sánchez and Torre Antón 2007). Applying this data to the Province of León, it gives a growth rate of 1.94% per year. This change was also analyzed comparing the maps from the First (1966) and Third (2006) National Forestry Inventories of Spain (NFI) for Province of León, while the Second NFI (1991) was not advisable to use. The comparison showed that approximately only 0.50% of the area was converted to forest each year, which is a more reliable measure. Furthermore, Table 4 (CI 100) gives a mean value for the area burned per year of 3% (changes from vegetated land covers to bare land). By contrast, official fire statistics from the Regional Government indicate that 1.98% of study area was burned each year, as an average for study period. These differences between our results and the reference data lead us to suggest that the amount of change was overestimated when based on the CI 100 maps.

Analysis of uncertainty

Figures 1 (b, c) and 3 (b, c) show that, after the application of filters based on confusion indices, the regional pattern of land cover remained similar, even if the number of available (unmasked) pixels decreased. However, more marked maxima and minima are evident in Figure 3 (b, c). The “noise” introduced by the uncertainty disappears after applying CI and the maps show a more realistic landscape pattern, in accordance with the phenological status of the vegetation. For example, as the image available for 1994 corresponds to the beginning of June (when forest canopy is not

511 completely developed), it causes high confusion between forest and shrubland. After
512 applying CI filters, misclassifications are reduced (which correspond mainly with pixels
513 of forests), and shrublands became more abundant.

514 The average transition matrices (Table 4, CI 75 and CI 50) showed less change
515 after filtering the uncertainty (14.61% and 7.84% the of unmasked area with CI 75 and
516 CI 50 maps, respectively). The six major changes accounted for 81.4% of the total
517 change with CI 75 maps, reaching 85.7% with CI 50, while unlikely transitions were
518 almost absent. Moreover, changes from shrubland to forests and those related to fire
519 events decrease in extent when analyzing CI 75 and CI 50 maps. Thus, more realistic
520 results are obtained when our results are compared with the forest growth rates given by
521 NFI and Gil Sánchez and Torre Antón (2007), and mean area burned extracted from the
522 official fire statistics. Nevertheless, against the benefits of this approach, an excessive
523 loss of pixels after applying CI thresholds could imply an underestimation of the extent
524 of real changes, which are known to have occurred. If the vast majority of the study area
525 is masked due to uncertainty, then the data are probably not sufficient to estimate land
526 change, which is important information to know.

527 Despite these differences in area estimates, the rate of change in relation to the
528 unmasked area (i.e. all pixels with CI 100 maps, 75% of each image with CI 75 and
529 50% with CI 50 maps), was consistent between all the analyses. As an example, Figure
530 5a illustrates how the change from shrubland to bare land (mainly fire events, the most
531 important change in controlling landscape dynamics) was significantly ($r^2>0.9$, $p<0.01$;
532 n=13) consistent as detected by CI 100, CI 75 and CI 50 maps. Inversely, Figure 5b
533 shows the change from bare land to shrubland (vegetation recovery after disturbance).
534 Again, the percentages provided by CI 100 maps were significantly correlated ($r^2>0.36$,
535 $p<0.01$; n=13) with CI 75 and CI 50 maps. Nevertheless, differences in the area

affected, prompted by the uncertainty assessment, were more important here than in Figure 5a. After one fire event, if the vegetation has time enough to recover until a certain level of biomass before the date of image acquisition, it will result in confusion. Thus, the most uncertainly classified pixels on CI 100 maps will be eliminated by the CI, and the changing area will be smaller. On the other hand, analyzing both figures together, quick recuperations appear after burning maxima (e.g. in 1994-1995), with rapid recovery rates during the subsequent two years (e.g. during 1995-1996 and 1996-1997). In fact, high correlations were found between fire events in shrublands at time *i* and vegetation recovery at time *i+1* and *i+2* (r^2>0.56, p<0.01; n=13). This indicates a short recovery period (i.e. between one and two years) for these communities after fire, in accordance with previous works (Calvo et al. 2002b; Lozano et al. 2007).

3.3 Landscape dynamics modelling

Modelling landscape dynamics identified “hot spots” affected by recurrence of disturbances and vegetation recovery patterns, which were also visible at a broad scale after applying confusion filters (Figure 6). A partial correlation was found between the higher recurrence values and longer times for vegetation recovery. Nonetheless, there were large differences throughout the area. Some areas with high resilience and a long history of anthropogenic disturbances, such as communities dominated by *Erica australis*, only needed one or two years to recover after a fire event (Calvo et al. 2002b), while others required more time. Whatever the reason for change, these differences might be related not only to patterns of fire recurrence and severity, or the previous stage of vegetation, but also to human factors, site history, climate and soil characteristics, which determinate the availability of nutrients, organic matter and other

properties (Roder et al. 2008; Serra et al. 2008; Vicente-Serrano et al. 2004). These driving factors are the most compelling research issues to investigate for modelling future landscape dynamics in the area.

Table 5 provides disturbance recurrence and recovery rates for the four major changes defined in Table 4 (i.e. transitions between forest-shrubland, and shrubland-bare land, in both directions of change), which have been modelled in this section. In general, the recurrence values varied between one and two. When the changes were analyzed after filtering uncertainty, or with the more secure *AA_BB* sequences, the recurrence values decreased significantly, showing a value of 1 with a low standard deviation. This could be explained by different reasons, depending on the change analyzed. The transition from forest to shrubland represents the most important change in terms of extent on study area (see Table 4). Nevertheless, it is highly unlikely to happen and it was related to misclassification effects, caused by succession phenomena on mixed pixels. On the other hand, the recurrence of change from shrubland to bare land may be interpreted as follows: (1) the majority of pixels classified as shrubland change to bare land only once or possibly twice during the study period (because of fire events and vegetation clearings), and (2) if shrub vegetation is eliminated by perturbations such as mines and quarries, it never recovers, so the recurrence of change is one, with no uncertainty.

In terms of vegetation recovery, results were more heterogeneous. The major change detected in extent was the transition from shrublands to forest (see Table 4). After filtering the uncertainty and analyzing the more secure sequences, the results were moderately realistic (e.g. a shrubland would need more than four years to evolve into a forest), probably as a consequence of the scale of the analyses and the effect of uncertainty. Therefore, further research is needed on study area for analyzing this land

586 cover change at a more detailed spatial scale. A comprehensive explanation for the
587 processes leading to land use and cover changes can only be achieved by combining
588 observations from different approaches. By contrast, changes from bare land to
589 shrubland gave interesting information. Working with sequences *A_B*, bare land needed
590 around two years to return to shrubland, with and without reducing classification
591 uncertainty. However, as Figure 6b shows, different situations may occur, ranging from
592 a recovery time of one year (e.g. areas where a small fire or in general low-severe
593 disturbance occurred) to thirteen years (i.e. mines and quarries established in areas
594 initially covered by shrubs, which never recover along study period). Furthermore, an
595 interesting effect appeared when more complex trajectories were explored (*AA_BB*
596 sequences). When bare land category persisted in the same place for more than one year
597 (two in this particular case), it is supposed that the disturbance which initially
598 eliminated the vegetation was more severe (e.g. strong fire severity), or that consecutive
599 disturbances occurred in a continuous basis (higher recurrence of fire events). This will
600 affect soil properties and, thus, it will potentially increase the time needed for vegetation
601 recovery. While 2.17 years were required on CI 100 maps with *A_B* sequences, 4.05
602 years were needed in *AA_BB* trajectories. This situation has been demonstrated in
603 previous works using other methodologies (Diaz-Delgado et al. 2002; Diaz-Delgado et
604 al. 2003), although the time required for recovery may also be related to the level of
605 complexity in the community affected by the disturbance (Calvo et al. 2002b).
606

607 ## 3.4 General discussion

608

609 The effects of uncertainty on inter-annual land cover changes have been
610 assessed. Patterns of change in the study area were consistent with and without masking

611 the most uncertain classified pixels. The vegetation has started to recover in disturbed
612 areas, although wildfires continue to occur. Those areas affected by higher recurrences
613 or more severe effects from disturbance required more time for vegetation recovery. But
614 at a global level, the rate of change decreased over time and a slow but continuous
615 homogenization of landscape occurred, although natural and socioeconomic driving
616 factors have not acted with the same intensity and direction of change over the whole
617 area.

618 Although we could never say that the present method eliminates uncertainty
619 because there will always be uncertainty, the patterns of land cover change were more
620 realistic after applying filters to the classified images based on CI thresholds, as
621 demonstrated previously. The CI was used to distinguish between a hard area,
622 containing relevant units, and an uncertain area, representing possible errors. The
623 number of available (unmasked) pixels decreased as those with the higher uncertainty
624 were removed. Consequently, the accuracy and coherence (i.e. similarity) of the
625 classified images increased substantially. This evidence is highly important for
626 measuring land dynamics in heterogeneous and resilient landscapes, using temporal
627 sequences of remotely sensed imagery (Roy 2000). If the datasets are not accurately
628 coregistered or misclassification errors significantly exaggerate or alternatively mask
629 change, the assessment of thematic accuracy would be hampered (Foody 2002), and any
630 difference observed over time may not be attributable solely, if at all, to real change on
631 the ground (Pontius and Lippitt 2006). In fact, a key concern is that thematic maps
632 derived from remotely sensed data are often judged to be of insufficient quality for
633 operational applications (Foody 2002), and usually tend to be poorly communicated to
634 the user (van Oort 2007; Shao and Wu 2008).

Nevertheless, against the benefits of this approach, the method is not able to detect whether some of the eliminated pixels are largely areas of true land cover change. The method can show how much of the study area contains a substantial amount of error, so we can distinguish data that might be useful to measure land change from data that are not particularly useful. For some case studies, there might be so much uncertainty that the method masks most of the map, which would be helpful to know; while other types of maps might have so little uncertainty that very little of the map becomes masked. In this way, an excessive loss of pixels could make change detection difficult, so underestimating the real extent of land cover change on the ground, while the direct use of hard classifications overestimate its magnitude. Thus, since land cover transitions are sensitive to the elimination of pixels that are highly uncertain, their elimination requires extreme caution (Story and Congalton 1986). Although the overall accuracy of confusion and transition matrices might be high enough to detect real changes between consecutive years, without increasing the effects due to errors (Fuller et al. 2003), this will always depend on the complexity of study area (Rogan et al. 2002) and the objectives of the analysis (Canters 1997; Janssen and van der Wel 1994).

4. Conclusions

The application of uncertainty analyses to high temporal resolution image series (at an annual scale) provides a useful tool to describe land cover dynamics in heterogeneous and resilient landscapes, which are affected by recurrent disturbances (such as fire events). Firstly, when studies on landscape change are carried out on the basis of simple classification products derived from few images spread over time, landscape dynamics could be miss-detected and, therefore, linking patterns to processes

660 may became unreliable. The rapid vegetation recoveries after fire found in the study
661 area would not be detected if the image data were not available for every year.
662 Secondly, if the research question does not go beyond determining the nature of general
663 changes or trends, the analysis of aggregated values obtained directly from Maxlike
664 would be an acceptable choice, on the basis of the consistent trends obtained with and
665 without the analysis of uncertainty. Nevertheless, when analyzing the rate of change,
666 frequency of disturbances (recurrence) or vegetation recovery times, the effects of
667 uncertainty must be eliminated to obtain trustworthy results. In this case, working
668 directly with the hard-classified images could seriously hamper our understanding of
669 reality.

670 Secure interpretation requires that the reader be cognizant with what the
671 proposed methods can and cannot accomplish. Although an excessive loss of pixels (or
672 information) hampers the accurate assessment of land cover change on the ground, the
673 approach, however, eliminates false positives and determines where a particular
674 transition takes place with higher levels of reliability. On the one hand, CI 100 maps
675 contain all land cover changes in the study area, but are severely affected by large areas
676 of error. By contrast, CI 75 and CI 50 maps can eliminate the majority of error as well
677 as real changes, if conversions occur where the maps tend to be uncertain. Following
678 this approach, and given information concerning the maps and their errors, our method
679 could quantify whether it is possible to determine the amount of change on the ground.
680 This requires work directed towards the search for a suitable CI threshold that provides
681 some level of equilibrium, maximizing the real land cover change and minimizing the
682 sources of error and uncertainty, by comparing results with reliable sources of ground
683 information.

684

Acknowledgements

This work was supported by the Regional Government of Junta de Castilla y León (Spain) and Fondo Social Europeo, under the research project funding supplied by the order EDU/1490/2003, awarded to J. M. Álvarez. The authors would like to thank their support and comments to Fire Ecology research group of the University of León, Land Dynamics group of the University of Wageningen, Cartography Support Service of the University of León and forest engineers and rangers of the Autonomous Region of Castilla y León. We also are grateful to Althea Davies, F.J. Lozano, A. Moran and L. Soler for help, and the anonymous reviewers for their helpful comments and information. Finally we wish to thank the Environmental Section of Junta de Castilla y León for their support to this study by providing digital geographical data.

References

Ahamed, T.R.N., Rao, K.G., and Murthy, J.S.R. (2000). GIS-based fuzzy membership model for crop-land suitability analysis. Agricultural Systems 63: 75-95

Benayas, J.M., Martins, A., Nicolau, J.M., and Schulz, J.J. (2007). Abandonment of agricultural land: an overview of drivers and consequences. In V.S. CAB Reviews: Perspectives in Agriculture, Nutrition and Natural Resources (Ed.)

Bradley, B.A., and Mustard, J.F. (2005). Identifying land cover variability distinct from land cover change: Cheatgrass in the Great Basin. Remote Sensing of Environment 94: 204-213

Burgi, M., Hersperger, A.M., and Schneeberger, N. (2004). Driving forces of landscape change - current and new directions. Landscape Ecology 19: 857-868

709 Burnicki, A.C., Brown, D.G., and Goovaerts, P. (2007). Simulating error propagation in
710 land-cover change analysis: The implications of temporal dependence. Computers,
711 Environment and Urban Systems 31: 282-302
712 Burrough, P.A., vanGaans, P.F.M., and Hootsmans, R. (1997). Continuous
713 classification in soil survey: Spatial correlation, confusion and boundaries. Geoderma
714 77: 115-135
715 Calvo, L., Tarrega, R., and de Luis, E. (1999). Post-fire succession in two Quercus
716 pyrenaica communities with different disturbance histories. Annals of Forest Science
717 56: 441-447
718 Calvo, L., Tarrega, R., and de Luis, E. (2002a). The dynamics of mediterranean shrubs
719 species over 12 years following perturbations. Plant Ecology 160: 25-42
720 Calvo, L., Tarrega, R., and de Luis, E. (2002b). Secondary succession after
721 perturbations in a shrubland community. Acta Oecologica-International Journal of
722 Ecology 23: 393-404
723 Canters, F. (1997). Evaluating the uncertainty of area estimates derived from fuzzy
724 land-cover classification. Photogrammetric Engineering and Remote Sensing 63: 403-
725 414
726 Carmel, Y. (2004). Characterizing location and classification error patterns in time-
727 series thematic maps. Geoscience and Remote Sensing Letters IEEE 1: 11-14
728 Carmel, Y., Dean, D.J., and C.D., Flather (2001). Combining location and classification
729 error sources for estimating multi-temporal database accuracy. Photogrammetric
730 Engineering and Remote Sensing 67: 865-872
731 Carvalho, d.L.M.T., Jan G. P. W. Clevers, Andrew K. Skidmore, and Jong, S.M.d.
732 (2004). Selection of imagery data and classifiers for mapping Brazilian semideciduous

733 Atlantic forests. International Journal of Applied Earth Observation and Geoinformation
734 5: 173-186
735 Cayuela, L., Benayas, J.M.R., and Echeverria, C. (2006). Clearance and fragmentation
736 of tropical montane forests in the Highlands of Chiapas, Mexico (1975-2000). Forest
737 Ecology and Management 226: 208-218
738 Conese, C., and Maselli, F. (1992). Use of Error Matrices to Improve Area Estimates
739 with Maximum-Likelihood Classification Procedures. Remote Sensing of Environment
740 40: 113-124
741 Congalton, R.G. (1991). A Review of Assessing the Accuracy of Classifications of
742 Remotely Sensed Data. Remote Sensing of Environment 37: 35-46
743 Chavez, P.S. (1996). Image-based atmospheric corrections revisited and improved.
744 Photogrammetric Engineering and Remote Sensing 62: 1025-1036
745 Cherrill, A., and McClean, C. (1995). An investigation of uncertainty in field habitat
746 mapping and the implications for detecting land cover change. Landscape Ecology 10:
747 5-21
748 Chuvieco, E. (2000). Fundamentos de Teledetección espacial. Madrid: EDICIONES
749 RIALP, S.A.
750 Dai, X.L., and Khorram, S. (1998). The effects of image misregistration on the accuracy
751 of remotelysensed change detection. IEEE Transactions on Geoscience and Remote
752 Sensing 36: 1566-1577
753 Diaz-Delgado, R., Lloret, F., Pons, X., and Terradas, J. (2002). Satellite evidence of
754 decreasing resilience in Mediterranean plant communities after recurrent wildfires.
755 Ecology 83: 2293-2303

Diaz-Delgado, R., Llorett, F., and Pons, X. (2003). Influence of fire severity on plant regeneration by means of remote sensing imagery. International Journal of Remote Sensing 24: 1751-1763

Diaz-Delgado, R., and Pons, X. (2001). Spatial patterns of forest fires in Catalonia (NE of Spain) along the period 1975-1995 - Analysis of vegetation recovery after fire. Forest Ecology and Management 147: 67-74

Duveiller, G., Defourny, P., Desclée, B., and Mayaux, P. (2008). Deforestation in Central Africa: Estimates at regional, national and landscape levels by advanced processing of systematically-distributed Landsat extracts. Remote Sensing of Environment 115: 1969-1981

Edwards, G., and Lowell, K.E. (1996). Modeling uncertainty in photointerpreted boundaries. Photogrammetric Engineering and Remote Sensing 62: 377-391

ERDAS (2001). ERDAS Imagine 8.5.

ESRI (2006). ArcGIS 9.2.

Foody, G.M. (1996). Approaches for the production and evaluation of fuzzy land cover classifications from remotely-sensed data. International Journal of Remote Sensing 17: 1317-1340

Foody, G.M. (2002). Status of land cover classification accuracy assessment. Remote Sensing of Environment 80: 185-201

Foody, G.M., and Boyd, D.S. (1999). Detection of partial land cover change associated with the migration of inner-class transitional zones. International Journal of Remote Sensing 20: 2723-2740

Fuller, R.M., Smith, G.M., and Devereux, B.J. (2003). The characterisation and measurement of land cover change through remote sensing: problems in operational

780 applications? International Journal of Applied Earth Observation and Geoinformation 4:
781 243-253
782 Gautam, A.P., Webb, E.L., Shivakoti, G.P., and Zoebisch, M.A. (2003). Land use
783 dynamics and landscape change pattern in a mountain watershed in Nepal. Agriculture
784 Ecosystems and Environment 99: 83-96
785 Gil Sánchez, C., and Torre Antón, M. (2007). Atlas forestal de Castilla y León, Junta de
786 Castilla y León, Consejería de Medio Ambiente, Valladolid.
787 Gilabert, M.A., Conese, C., and Maselli, F. (1994). An Atmospheric Correction Method
788 for the Automatic Retrieval of Surface Reflectances from Tm Images. International
789 Journal of Remote Sensing 15: 2065-2086
790 Janssen, L.L.F., and Van der Vel, F.J.M. (1994). Accuracy assessment of satellite
791 derived land-cover data: a review. Photogrammetric Engineering and Remote Sensing
792 60: 419-426
793 Janssen, L.L.F., and van der Wel, F.J.M. (1994). Accuracy assessment of satellite
794 derived land-cover data: a review. Photogrammetric Engineering and Remote Sensing
795 60: 419-426
796 Kauth, R.J., and Thomas, G.S. (1976). The Tasseled Cap. A Graphic Description of the
797 Spectral-Temporal Development of Agricultural Crops as Seen by LANDSAT. In,
798 Symposium on Machine Processing of Remotely Sensed Data (pp. 4B-41 to 44B-51).
799 Purdue University of West Lafayette, Indiana
800 Lambin, E.F. (1999). Monitoring forest degradation in tropical regions by remote
801 sensing: some methodological issues. Global Ecology and Biogeography 8: 191-198
802 Lambin, E.F., Turner, B.L., Geist, H.J., Agbola, S.B., Angelsen, A., Bruce, J.W.,
803 Coomes, O.T., Dirzo, R., Fischer, G., Folke, C., George, P.S., Homewood, K.,
804 Imbernon, J., Leemans, R., Li, X.B., Moran, E.F., Mortimore, M., Ramakrishnan, P.S.,

805 Richards, J.F., Skanes, H., Steffen, W., Stone, G.D., Svedin, U., Veldkamp, T.A.,
806 Vogel, C., and Xu, J.C. (2001). The causes of land-use and land-cover change: moving
807 beyond the myths. Global Environmental Change-Human and Policy Dimensions 11:
808 261-269
809 Lewis, H.G., Brown, M., and Tatnall, A.R.L. (2000). Incorporating uncertainty in land
810 cover classification from remote sensing imagery. Remote Sensing for Land Surface
811 Characterisation 26: 1123-1126
812 Lillesand, T.M., Kiefer, R.W., and Chipman, J.W. (2008). Remote Sensing and Image
813 Interpretation: John Wiley and Sons
814 Liu, C.R., Frazier, P., and Kumar, L. (2007). Comparative assessment of the measures
815 of thematic classification accuracy. Remote Sensing of Environment 107: 606-616
816 Lozano, F.J., Suárez-Seoane, S., and de Luis, E. (2007). Estudio comparativo de los
817 regímenes de fuego en tres espacios naturales protegidos del oeste peninsular mediante
818 imágenes Landsat. Revista Española de Teldetección. Accepted
819 Lozano, F.J., Suarez-Seoane, S., Kelly, M., and Luis, E. (2008). A multi-scale approach
820 for modeling fire occurrence probability using satellite data and classification trees: A
821 case study in a mountainous Mediterranean region. Remote Sensing of Environment
822 112: 708-719
823 Lloret, F., Calvo, E., Pons, X., and Diaz-Delgado, R. (2002). Wildfires and landscape
824 patterns in the Eastern Iberian peninsula. Landscape Ecology 17: 745-759
825 MacDonald, D., Crabtree, J.R., Wiesinger, G., Dax, T., Stamou, N., Fleury P., Gutierrez
826 Lazpita, J.a., and Gibon, A. (2000). Agricultural abandonment in mountain areas of
827 Europe: Environmental consequences and policy response. Journal of Environmental
828 Management 59: 47-69

829 Markham, B.L., and Barker, J.L. (1987). Radiometric Properties of United-States
830 Processed Landsat Mss Data. Remote Sensing of Environment 22: 39-71
831 Martin, M.E., Newman, S.D., Aber, J.D., and Congalton, R.G. (1998). Determining
832 forest species composition using high spectral resolution remote sensing data. Remote
833 Sensing of Environment 65: 249-254
834 Metternicht, G.I. (2003). Categorical fuzziness: a comparison between crisp and fuzzy
835 class boundary modelling for mapping salt-affected soils using Landsat TM data and a
836 classification based on anion ratios. Ecological Modelling 168: 371-389
837 Moran, M.S., Jackson, R.D., Slater, P.N., and Teillet, P.M. (1992). Evaluation of
838 Simplified Procedures for Retrieval of Land Surface Reflectance Factors from Satellite
839 Sensor Output. Remote Sensing of Environment 41: 169-184
840 Ninyerola, M., Pons, X., and Roure, J.M. (2005). Atlas Climático Digital de la
841 Península Ibérica. Metodología y aplicaciones en bioclimatología y geobotánica. ISBN
842 932860-8-7. Universidad Autónoma de Barcelona, Bellaterra
843 Owen, S.M., MacKenzie, A.R., Bunce, R.G.H., Stewart, H.E., Donovan, R.G., Stark,
844 G., and Hewitt, C.N. (2006). Urban land classification and its uncertainties using
845 principal component and cluster analyses: A case study for the UK West Midlands.
846 Landscape and Urban Planning 78: 311-321
847 Pala, V., and Pons, X. (1995). Incorporation of Relief in Polynomial-Based Geometric
848 Corrections. Photogrammetric Engineering and Remote Sensing 61: 935-944
849 Pontius, R.G., and Lippitt, C.D. (2006). Can Error Explain Map Differences Over
850 Time? Cartography and Geographic Information Science 33: 159-171
851 Pontius, R.G., Shusas, E., and McEachern, M. (2004). Detecting important categorical
852 land changes while accounting for persistence. Agriculture Ecosystems and
853 Environment 101: 251-268

854 Rees, W.G., Williams, M., and Vitebsky, P. (2003). Mapping land cover change in a
855 reindeer herding area of the Russian Arctic using Landsat TM and ETM+ imagery and
856 indigenous knowledge. Remote Sensing of Environment 85: 441-452
857 Riaño, D., Chuvieco, E., Salas, J., and Aguado, I. (2003). Assessment of different
858 topographic corrections in Landsat-TM data for mapping vegetation types (2003). IEEE
859 Transactions on Geoscience and Remote Sensing 41: 1056-1061
860 Roder, A., Hill, J., Duguy, B., Alloza, J.A., and Vallejo, R. (2008). Using long time
861 series of Landsat data to monitor fire events and post-fire dynamics and identify driving
862 factors. A case study in the Ayora region (eastern Spain). Remote Sensing of
863 Environment 112: 259-273
864 Rogan, J., Franklin, J., and Roberts, D.A. (2002). A comparison of methods for
865 monitoring multitemporal vegetation change using Thematic Mapper imagery. Remote
866 Sensing of Environment 80: 143-156
867 Rollings, M. G., R. E. Keane and R. A. Parsons (2004) Mapping fuels and fire regimes
868 using remote sensing, ecosystem simulation and gradient modeling. Ecological
869 Applications 14: 75-95.
870 Rouse, J.W., Haas, R.H., Schell, J.A., and Deering, D.W. (1973). Monitoring vegetation
871 systems in the Great Plains with ERTS. In NASA (Ed.), Third ERTS Symposium (pp.
872 309-317)
873 Roy, D.P. (2000). The impact of misregistration upon composited wide field of view
874 satellite data and implications for change detection. IEEE Transactions on Geoscience
875 and Remote Sensing 38: 2017-2032
876 Serra, P., Pons, X., and Saurí, D. (2008). Land-cover and land-use change in a
877 Mediterranean landscape: A spatial analysis of driving forces integrating biophysical
878 and human factors. Applied Geography 28: 189-209

879 Shalaby, A., and Tateishi, R. (2007). Remote sensing and GIS for mapping and
880 monitoring land cover and land-use changes in the Northwestern coastal zone of Egypt.
881 Applied Geography 27: 28-41
882 Shao G. and Wu J. 2008. On the accuracy of landscape pattern analysis using remote
883 sensing data. Landscape Ecology 23: 505-511.
884 Steele, B.M., Winne, J.C., and Redmond, R.L. (1998). Estimation and Mapping of
885 Misclassification Probabilities for Thematic Land Cover Maps. Remote Sensing of
886 Environment 66: 192-202
887 Stehman, S.V. (1997). Selecting and interpreting measures of thematic classification
888 accuracy. Remote Sensing of Environment 62: 77-89
889 Stehman, S.V., and Czaplewski, R.L. (1998). Design and analysis for thematic map
890 accuracy assessment: Fundamental principles. Remote Sensing of Environment 64: 331-
891 344
892 Stoorvogel, J.J., and Antle, J.M. (2001). Regional land use analysis: the development of
893 operational tools. Agricultural Systems 70: 623-640
894 Story, M., and Congalton, R.G. (1986). Accuracy Assessment - a Users Perspective.
895 Photogrammetric Engineering and Remote Sensing 52: 397-399
896 Tapia, R., Stein, A., and Bijker, W. (2005). Optimization of sampling schemes for
897 vegetation mapping using fuzzy classification. Remote Sensing of Environment 99:
898 425-433
899 Teillet, P.M. (1986). Image Correction for Radiometric Effects in Remote-Sensing.
900 International Journal of Remote Sensing 7: 1637-1651
901 Thomlinson, J.R., Bolstad, P.V., and Cohen, W.B. (1999). Coordinating Methodologies
902 for Scaling Landcover Classifications from Site-Specific to Global: Steps toward
903 Validating Global Map Products. Remote Sensing of Environment 70: 16-28

Treitz, P., and Rogan, J. (2004). Remote sensing for mapping and monitoring land-cover and land-use change-an introduction. Progress in Planning 61: 269-279

Triepke, F.J., Brewer, C.K., Leavell, D.M., and Novak, S.J. (2008). Mapping forest alliances and associations using fuzzy systems and nearest neighbor classifiers. Remote Sensing of Environment 112: 1037-1050

van Oort, P.A.J. (2007). Interpreting the change detection error matrix. Remote Sensing of Environment 108: 1-8

Veldkamp, A., and Fresco, L.O. (1997). Reconstructing land use drivers and their spatial scale dependence for Costa Rica (1973 and 1984). Agricultural Systems 55: 19-43

Verburg, P.H., Soepboer, W., Veldkamp, A., Limpiada, R., Espaldon, V., and Mastura, S.S.A. (2002). Modeling the spatial dynamics of regional land use: The CLUE-S model. Environmental Management 30: 391-405

Vicente-Serrano, S.M., Lasanta, T., and Romo, A. (2004). Analysis of Spatial and Temporal Evolution of Vegetation Cover in the Spanish Central Pyrenees: Role of Human Management. Environmental Management 34: 802-818

Wang, M.H., and Howarth, P.J. (1993). Modeling Errors in Remote-Sensing Image Classification. Remote Sensing of Environment 45: 261-271

Wilson, E.H., and Sader, S.A. (2002). Detection of forest harvest type using multiple dates of Landsat TM imagery. Remote Sensing of Environment 80: 385-396

Woodcock, C.E., and Gopal, S. (2000). Fuzzy set theory and thematic maps: accuracy assessment and area estimation. International Journal of Geographical Information Science 14: 153-172

927 Xiao, J.Y., Shen, Y.J., Ge, J.F., Tateishi, R., Tang, C.Y., Liang, Y.Q., and Huang, Z.Y.
928 (2006). Evaluating urban expansion and land use change in Shijiazhuang, China, by
929 using GIS and remote sensing. Landscape and Urban Planning 75: 69-80
930 Zhang, J., and Foody, G.M. (1998). A fuzzy classification of sub-urban land cover from
931 remotely sensed imagery. International Journal of Remote Sensing 19: 2721-2738
932

933 Table 1. Image series used in land cover classification, with date of acquisition, sensor
934 type and solar elevation angle (degrees).

Image Date	Sensor type	Sun Angle
04/08/1991	TM	54.15
06/08/1992	TM	53.49
09/08/1993	TM	52.89
09/06/1994	TM	58.75
15/08/1995	TM	48.87
02/09/1996	TM	46.35
19/07/1997	TM	57.88
08/09/1998	TM	47.42
01/07/1999	ETM	63.03
05/09/2000	ETM	49.45
08/09/2001	ETM	48.39
27/09/2002	ETM	42.22
05/08/2003	TM	55.89
24/09/2004	TM	42.72

935

936 Table 2. Accuracy assessment of supervised classification for the validation years

937 (number of validation points)

	ground information						
2004 classification	Forest	Meadow	Shrubland	Rock	Bare	TOTAL	user´s accuracy
Forest	**324**	27	7	3	0	361	89.75%
Meadow	4	**207**	0	2	0	213	97.18%
Shrubland	21	12	**341**	14	2	390	87.44%
Rock	0	3	1	**219**	3	226	96.90%
Bare	1	1	1	62	**70**	135	51.85%
TOTAL	350	250	350	300	75	**1325**	
producer´s accuracy	92.57%	82.80%	97.43%	73.00%	93.33%		**88%**
2000 classification	Forest	Meadow	Shrubland	Rock	Bare	TOTAL	user´s accuracy
Forest	**45**	0	3	0	0	48	93.75%
Meadow	0	**48**	0	0	0	48	100.00%
Shrubland	5	1	**91**	0	1	98	92.86%
Rock	0	1	2	**40**	2	45	88.89%
Bare	0	0	4	10	**47**	61	77.05%
TOTAL	50	50	100	50	50	**300**	
producer´s accuracy	90.00%	96.00%	91.00%	80.00%	94.00%		**90%**
1997 classification	Forest	Meadow	Shrubland	Rock	Bare	TOTAL	user´s accuracy
Forest	**45**	1	2	1	0	49	91.63%
Meadow	1	**48**	0	0	0	49	97.97%
Shrubland	4	0	**93**	2	13	112	82.79%
Rock	0	1	4	**42**	0	47	89.36%
Bare	0	0	1	5	**37**	43	85.94%
TOTAL	50	50	100	50	50	**300**	
producer´s accuracy	90.00%	96.03%	93.00%	83.81%	73.33%		**88%**
1991 classification	Forest	Meadow	Shrubland	Rock	Bare	TOTAL	user´s accuracy
Forest	**47**	5	0	0	1	53	88.68%
Meadow	0	**39**	0	0	0	39	100.00%
Shrubland	3	5	**91**	7	7	113	80.53%
Rock	0	1	4	**33**	8	46	71.74%
Bare	0	0	5	10	**34**	49	69.39%
TOTAL	50	50	100	50	50	**300**	
producer´s accuracy	94.00%	78.00%	91.00%	66.00%	68.00%		**81%**

938 Table 3. Overall accuracies of: (a) land cover maps, validated by accuracy assessment,
939 and (b) land cover change maps, created by comparing the validated land cover maps.
940 Analyses were done with all pixels classified by maximum likelihood (CI 100) and after
941 the application of the corresponding filters of confusion index (CI 75 and CI 50), to
942 eliminate the uncertainty associated with misclassification.

a)	overall accuracy of maps		
land cover map	CI 100	CI 75	CI 50
2004	88%	90.00%	90.00%
2000	90%	93.00%	95.00%
1997	88%	92.00%	95.00%
1991	81%	84.00%	90.00%

b)	overall accuracy of change maps		
land cover change map	CI 100	CI 75	CI 50
2000-2004	79.20%	83.70%	85.50%
1997-2000	79.20%	85.56%	90.25%
1991-1997	71.28%	77.28%	85.50%

943

Table 4. Average transition matrices for all pair-wise images through the study period, considering the analysis of uncertainty. Percentage of constant land cover is shown in parentheses and major changes in bold. Averaged gains and losses, as percentage of the area, are also shown.

CI 100	year *i+1*					Total year *i+1*	Gross loss
	Forest	Meadow	Shrubland	Rock	Bare		
year *i*							
Forest	(21.08)	0.58	**3.70**	0.22	0.13	25.71	4.63
Meadow	0.54	(3.99)	0.53	0.22	0.19	5.47	1.48
Shrubland	**3.76**	0.47	(44.08)	1.77	**2.68**	52.76	8.68
Rock	0.23	0.24	1.84	(4.97)	0.42	7.7	2.73
Bare	0.10	0.22	**2.90**	0.56	(4.58)	8.36	3.78
Total year *i*	25.71	5.5	53.05	7.74	8,00	100.00	21.3
Gross gain	4.63	1.51	8.97	2.77	3.42	21.3	

CI 75	year *i+1*					Total year *i+1*	Gross loss
	Forest	Meadow	Shrubland	Rock	Bare		
year *i*							
Forest	(25.40)	0.36	**2.81**	0.13	0.09	28.79	3.39
Meadow	0.33	(3.81)	0.26	0.16	0.11	4.67	0.86
Shrubland	**2.77**	0.24	(45.87)	1.12	**2.33**	52.33	6.46
Rock	0.12	0.17	0.99	(5.43)	0.23	6.94	1.51
Bare	0.05	0.12	**1.88**	0.34	(4.87)	7.26	2.39
Total year *i*	28.8	4.67	52.32	6.95	7.25	100.00	14.61
Gross gain	3.27	0.89	5.94	1.75	2.76	14.61	

CI 50	year *i+1*					Total year *i+1*	Gross loss
	Forest	Meadow	Shrubland	Rock	Bare		
year *i*							
Forest	(32.68)	0.15	**1.77**	0.05	0.05	34.7	2.02
Meadow	0.14	(3.55)	0.08	0.08	0.04	3.89	0.34
Shrubland	**1.71**	0.08	(45.98)	0.48	**1.66**	49.91	3.93
Rock	0.05	0.09	0.31	(5.35)	0.10	5.9	0.55
Bare	0.02	0.04	**0.78**	0.16	(4.61)	5.61	1,00
Total year *i*	34.7	3.89	49.9	5.90	5.61	100.00	7.84
Gross gain	1.92	0.36	2.94	0.77	1.85	7.84	

949 Table 5. Averaged recurrence of changes (in number of occurrences) and time needed
950 for restoration (in years) between the most important changes found on study area.
951 Standard deviations are shown in parentheses. Modelling was done with all pixels
952 classified by maximum likelihood (CI 100) and after the application of the
953 corresponding filters of confusion index (CI 75 and CI 50), to reduce the uncertainty
954 associated with misclassification. Land cover sequences *A_B* and *AA_BB* are assessed.

Changed from (*A*)	Changed to (*B*)	Sequence	CI 100	CI 75	CI 50
			RECURRENCE		
Forest	Shrubland	*A_B*	1.89 (1.02)	1.56 (0.88)	1.29 (0.66)
		AA_BB	1.07 (0.25)	1.06 (0.24)	1.02 (0.15)
Shrubland	Bare land	*A_B*	1.4 (0.68)	1.19 (0.46)	1.13 (0.38)
		AA_BB	1.04 (0.19)	1.02 (0.15)	1.01 (0.07)
			TIME FOR RESTORATION		
Shrubland	Forest	*A_B*	2.96 (2.94)	2.34 (2.94)	1.74 (2.38)
		AA_BB	4.69 (2.92)	4.51 (2.97)	4.13 (2.88)
Bare land	Shrubland	*A_B*	2.17 (1.95)	1.84 (1.88)	1.69 (1.95)
		AA_BB	4.05 (2.62)	3.41 (2.53)	2.96 (2.47)

955

956

Figure 1. Images of the study area for the start and end years of the series (1991 and 2004). (a) All pixels classified by maximum likelihood (CI 100). (b, c) 75% and 50% of the unmasked pixels after the application of the corresponding filters of confusion index (CI 75 and CI 50), to reduce the uncertainty associated with misclassification

Figure 2. Confusion index map for the classified image from 2004. CI 75 and CI 50 maps, where 75% and 50% of the image pixels remains unmasked, respectively, after the application of both CI thresholds, are also shown

Figure 3. Temporal evolution (% area occupied) of each land cover class, in relation to the % of unmasked area. (a) All pixels classified by maximum likelihood (CI 100). (b, c) 75% and 50% of the pixels remaining after the application of the corresponding filters of confusion index (CI 75 and CI 50) to mask the uncertainty associated with misclassification

Figure 4. Change image between 1999 and 2000. (a) All pixels classified by maximum likelihood (CI 100). (b, c) 75% and 50% of the pixels remaining after the application of the corresponding filters of confusion index (CI 75 and CI 50), to mask the uncertainty associated with misclassification

Figure 5. Percentage of area changed, in relation to unmasked area, from: (a) shrubland to bare land (burned areas), and (b) bare land to shrubland (vegetation recovery after fire), for all pairs of consecutive years. Analyses were done with all pixels classified by maximum likelihood (CI 100) and after the application of the corresponding filters of confusion index (CI 75 and CI 50), to mask the uncertainty associated with misclassification

Figure 6. Landscape dynamics modelling between shrublands and bare land: (a) disturbance recurrence (in number of times), (b) vegetation recovery (in years).

Analyses were done with all pixels classified by maximum likelihood (CI 100 maps), and with 75% least uncertain pixels (CI 75 maps), but interpolating results obtained with the Nearest Neighbour algorithm for creating continuous maps for the whole study area

987 Figure 1.

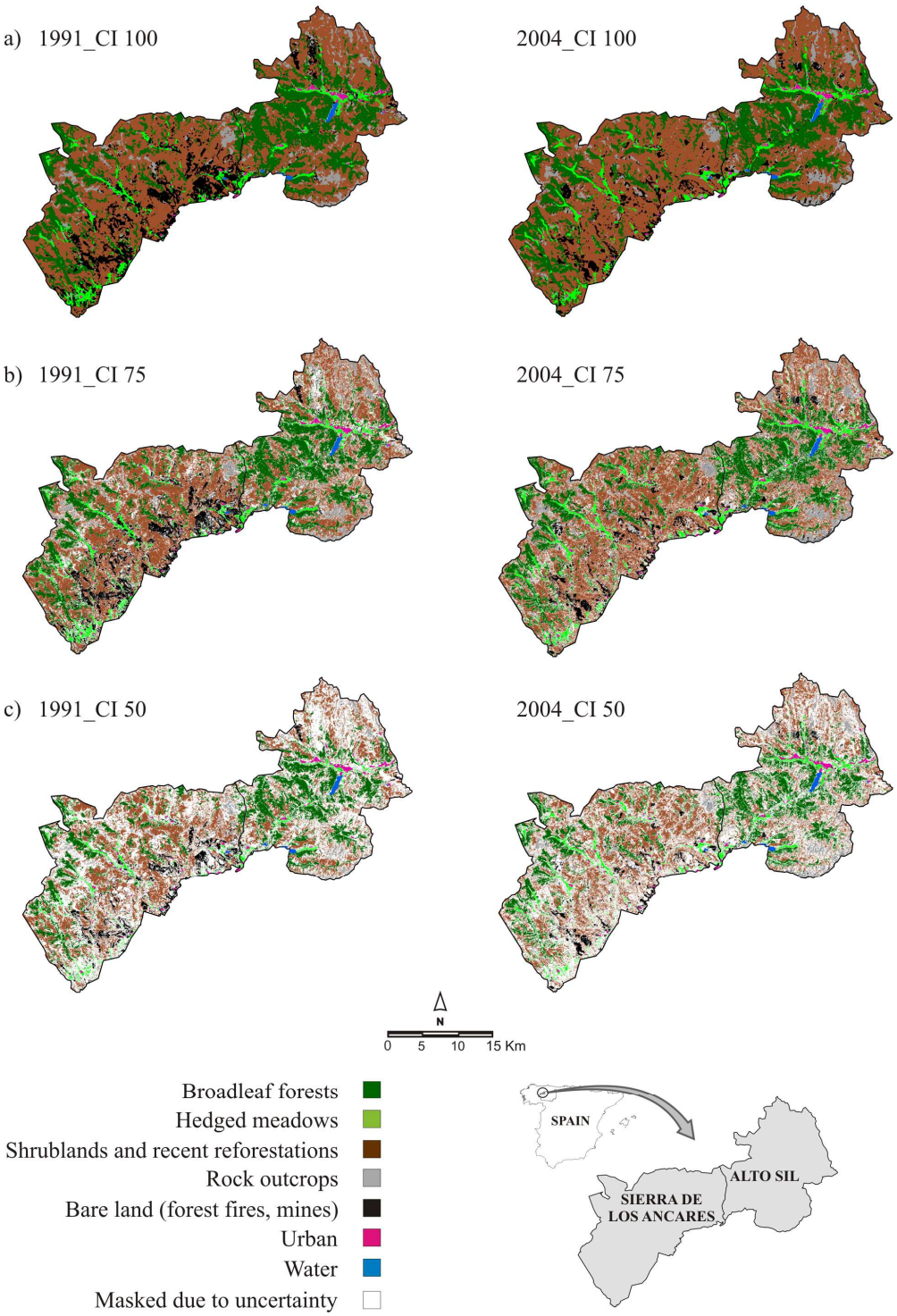

988

989 Figure 2.

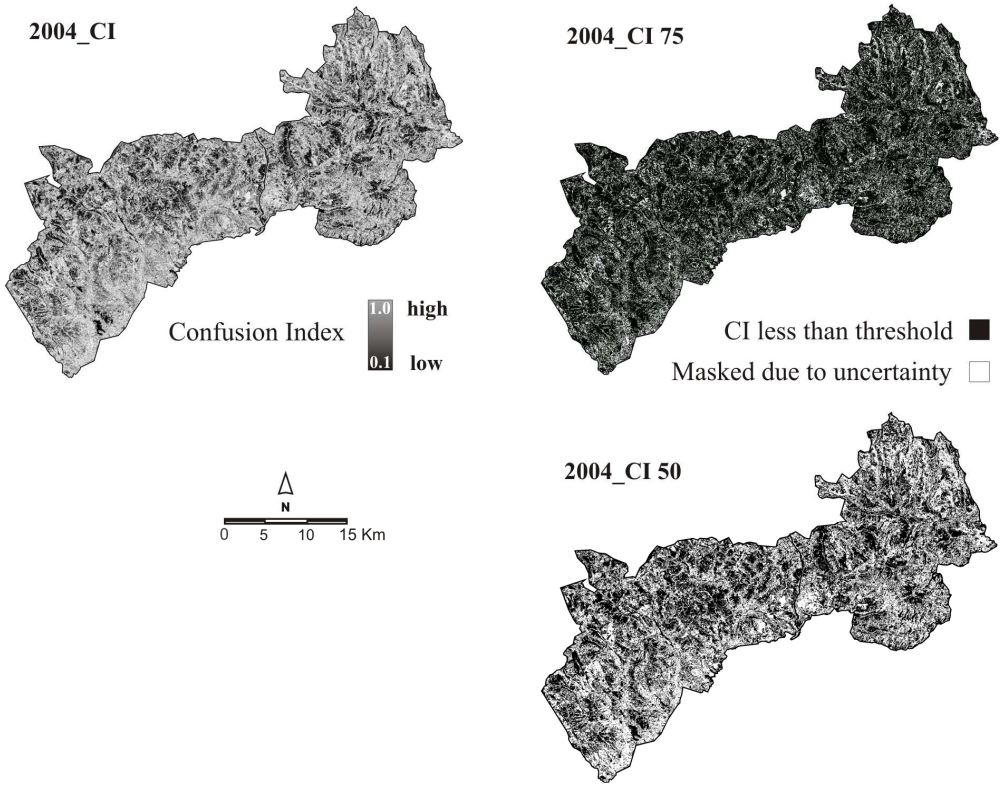

990

991 Figure 3.

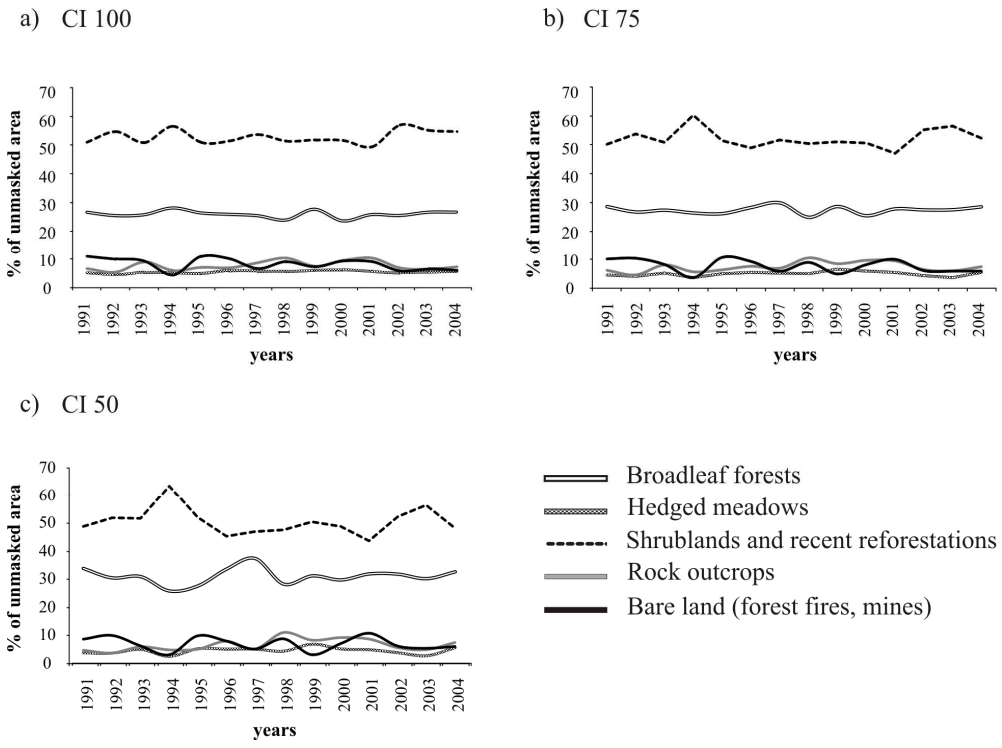

992

993 Figure 4.

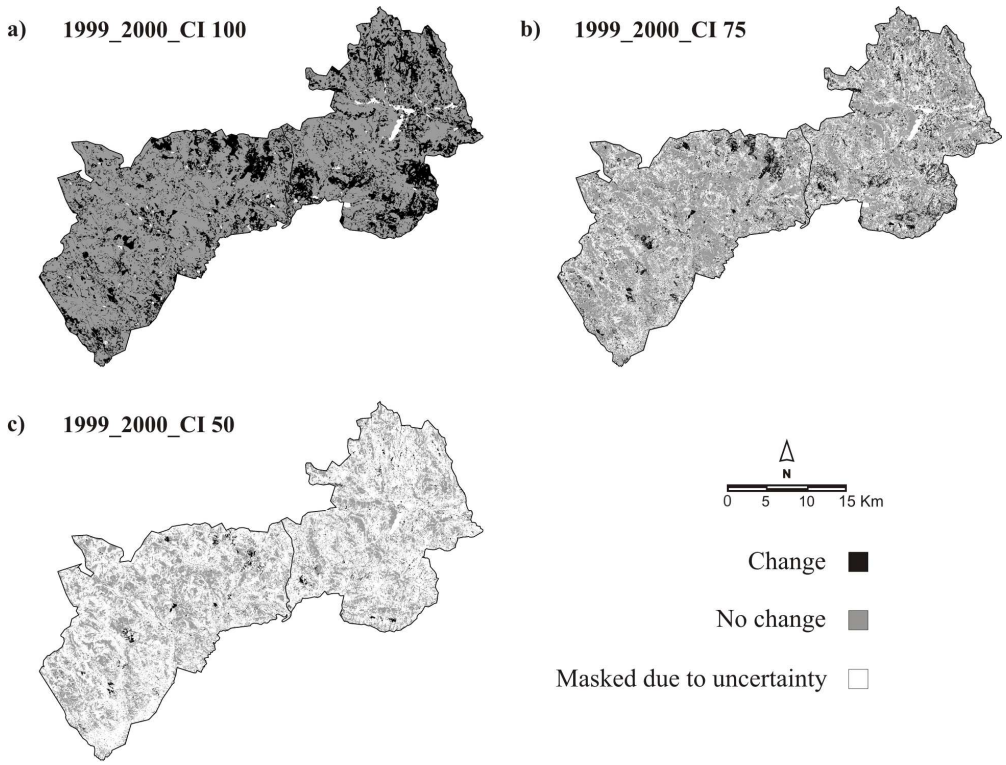

994

995 Figure 5.

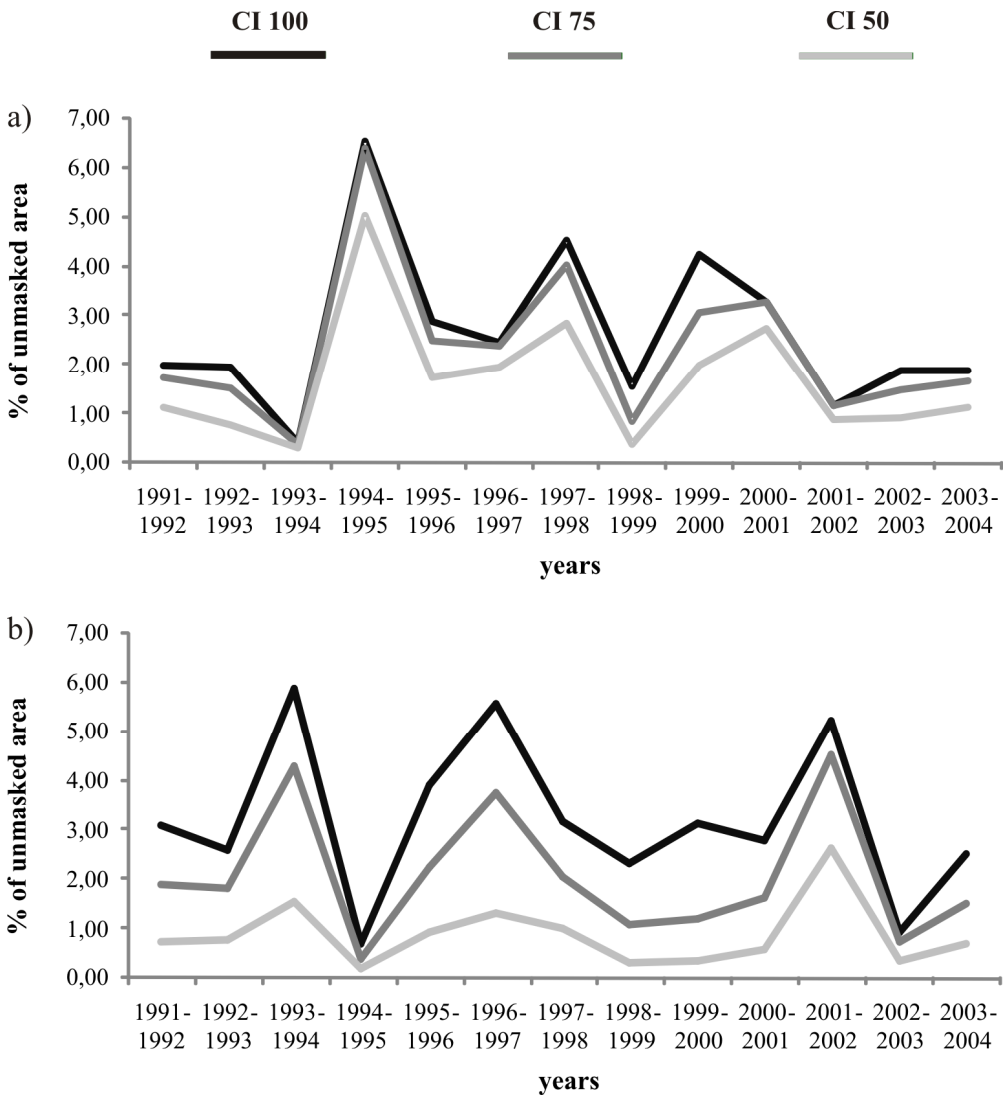

996

997 Figure 6.

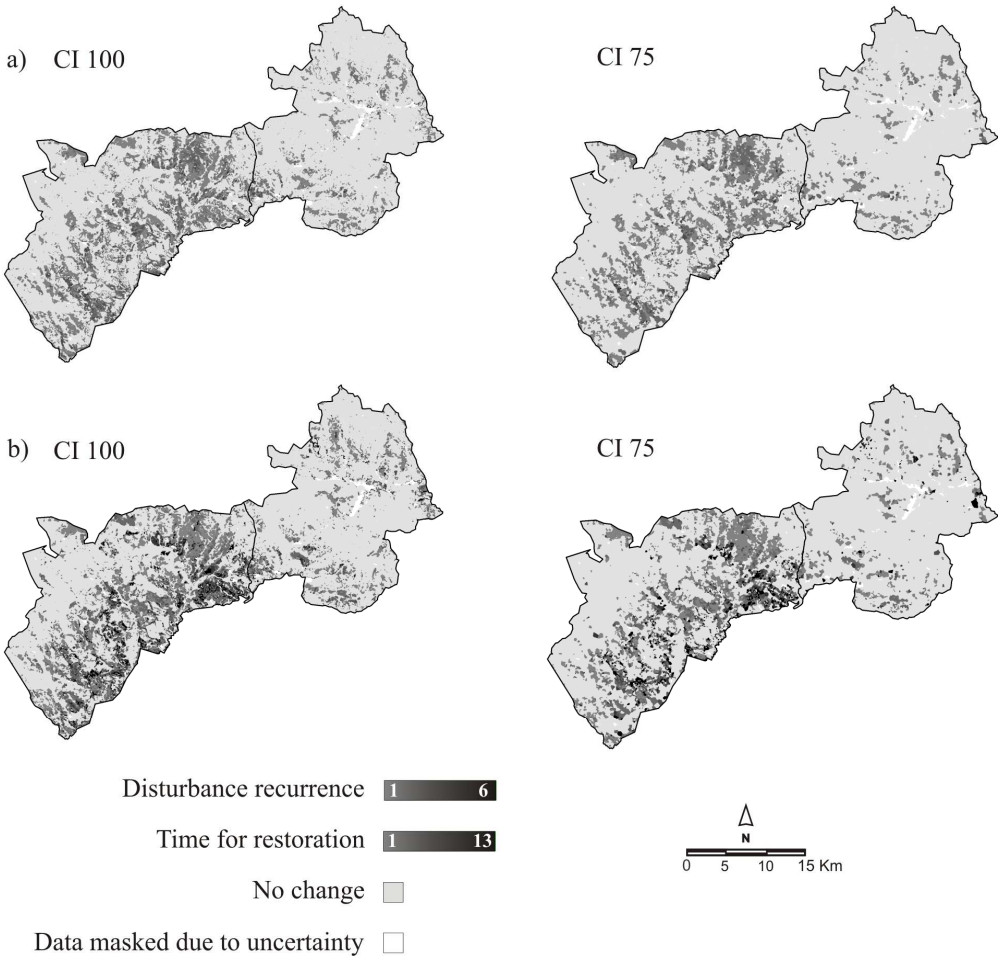

998

999